

Supporting Information For

Polymorphism, phase transition and physicochemical properties investigation of Ensifentrine

*Ananya Kar,^a Lopamudra Giri, ^{*b} Gowtham Kenguva,^a Smruti Rekha Rout^a, and Rambabu Dandela^{*a}*

^aDepartment of Industrial and Engineering Chemistry, Institute of Chemical Technology-
Indian Oil Bhubaneswar Campus, Bhubaneswar, India. E-mail:

r.dandela@iocb.ictmumbai.edu.in

^bDepartment of Chemistry, Odisha University of Technology and Research, (Formerly CET),
Bhubaneswar, India. E-mail: lopamudra7giri@gmail.com

Contents
Figure S1. PXRD patterns of Form I.
Figure S2. PXRD patterns of Form II.
Figure S3. PXRD patterns of Form III.
Table S1. Distinctive X-Ray Diffraction Peaks in ENSE Polymorphs.
Figure S4. Illustration of the formation of distinct forms under varied reaction environments. (a) rotary evaporation, (b) liquid-assisted grinding (LAG) and (c) LAG followed by slow-evaporation.
Figure S5. FT-IR spectra of various forms of ENSE.
Figure S6. ¹ H Spectra of (a) Form I, (b) Form II, and (c) Form III.
Figure S7. ¹³ C Spectra of (a) Form I, (b) Form II, and (c) Form III.
Figure S8. ¹ H spectra overlay of all ENSE forms.

Figure S9. ^{13}C spectra overlay of all ENSE forms.

Figure S10. TGA profiles of various forms of ENSE.

Details of the solubility parameters of solid forms of ENSE

Figure S11. ORTEP view of ENSE.Cl Salt. Herein, the ellipsoids are drawn with a 50% probability.

Table S2. Crystallographic Parameters of ENSE.Cl.Salt.

Figure S12. After the solubility test, a comparative PXRD overlay of all the solid forms of ENSE showed the production of discrete, stable adducts that matched the simulated pattern of ENSE.Cl Salt.

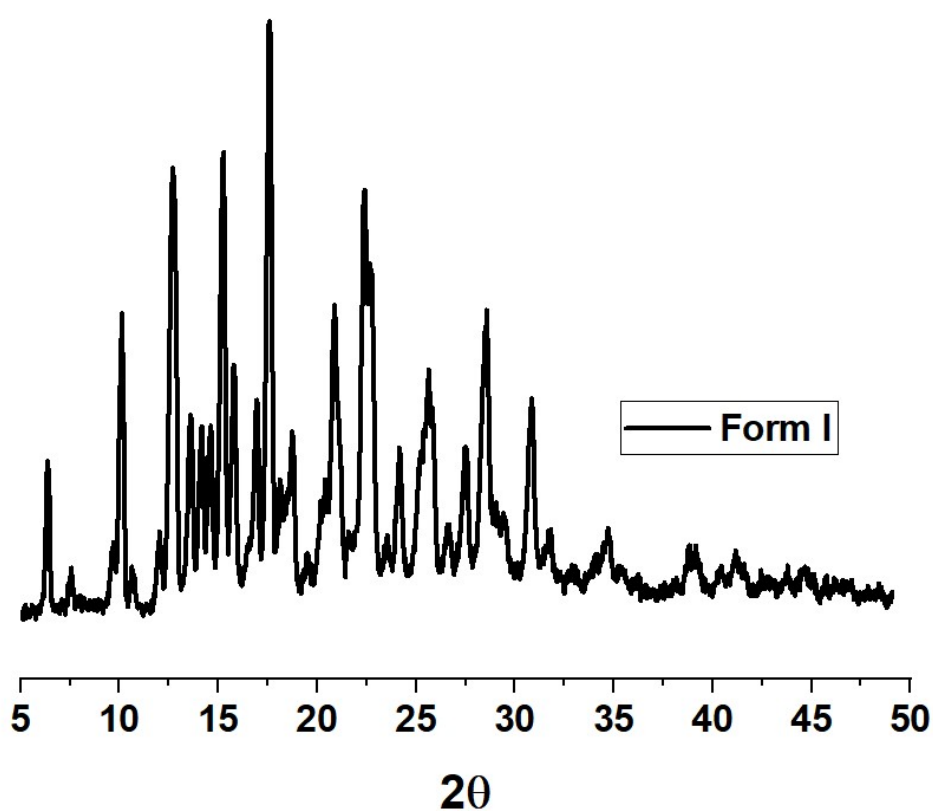


Figure S1. PXRD patterns of Form I.

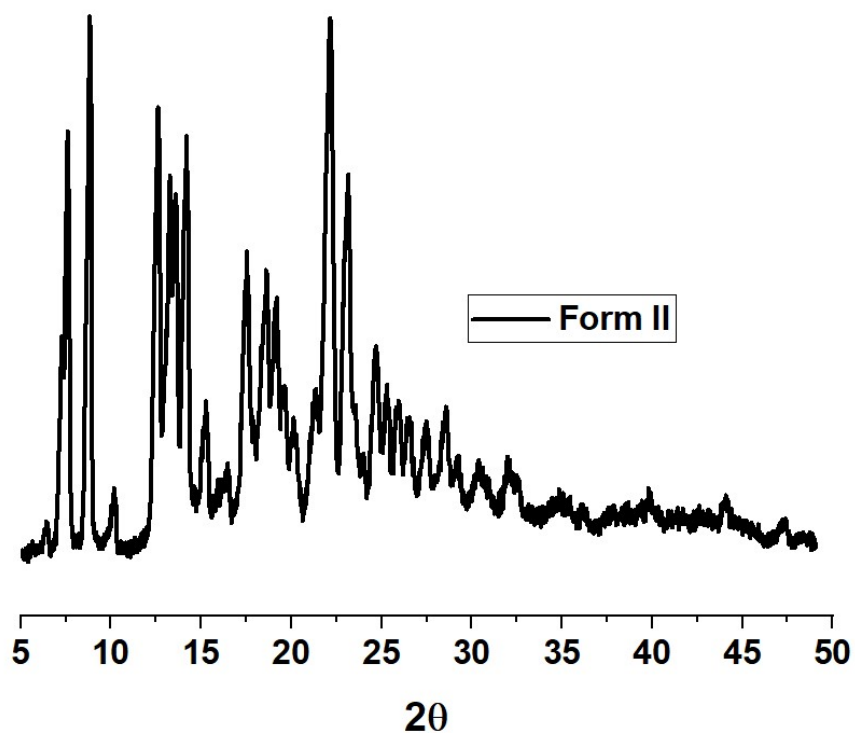


Figure S2. PXRD patterns of Form II.

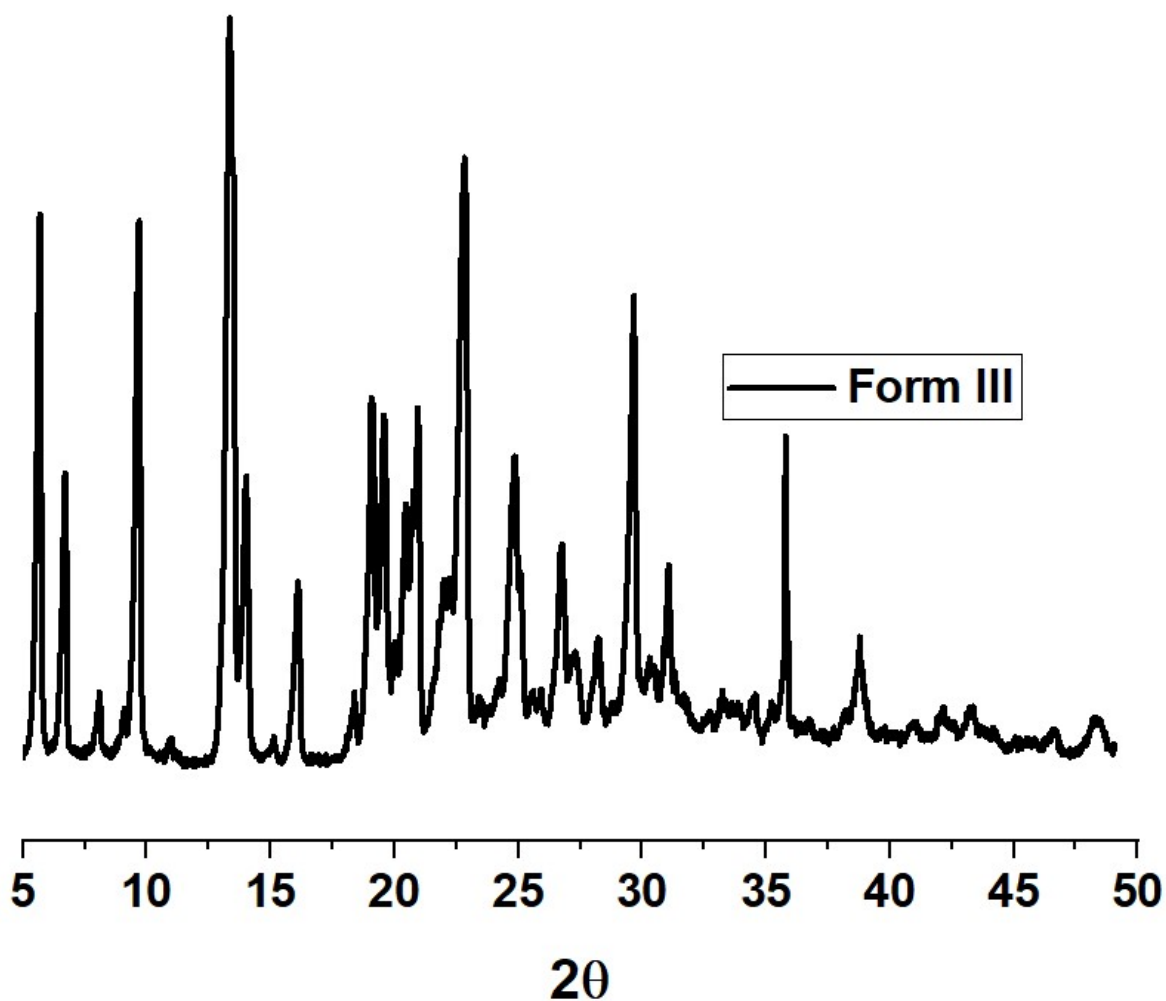
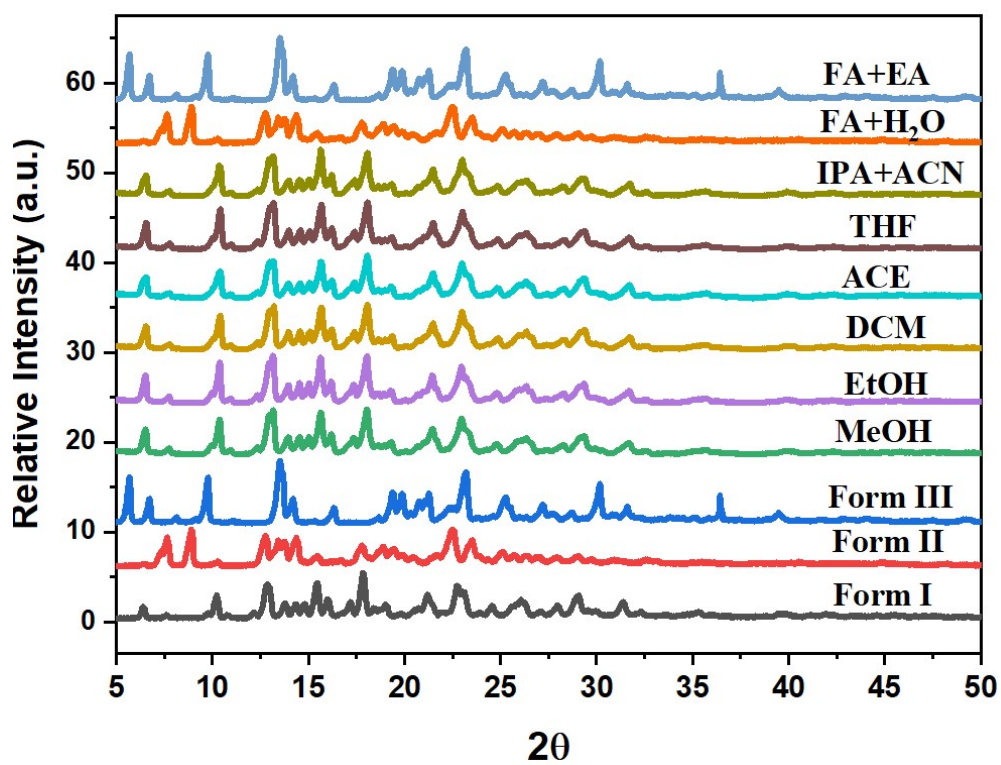


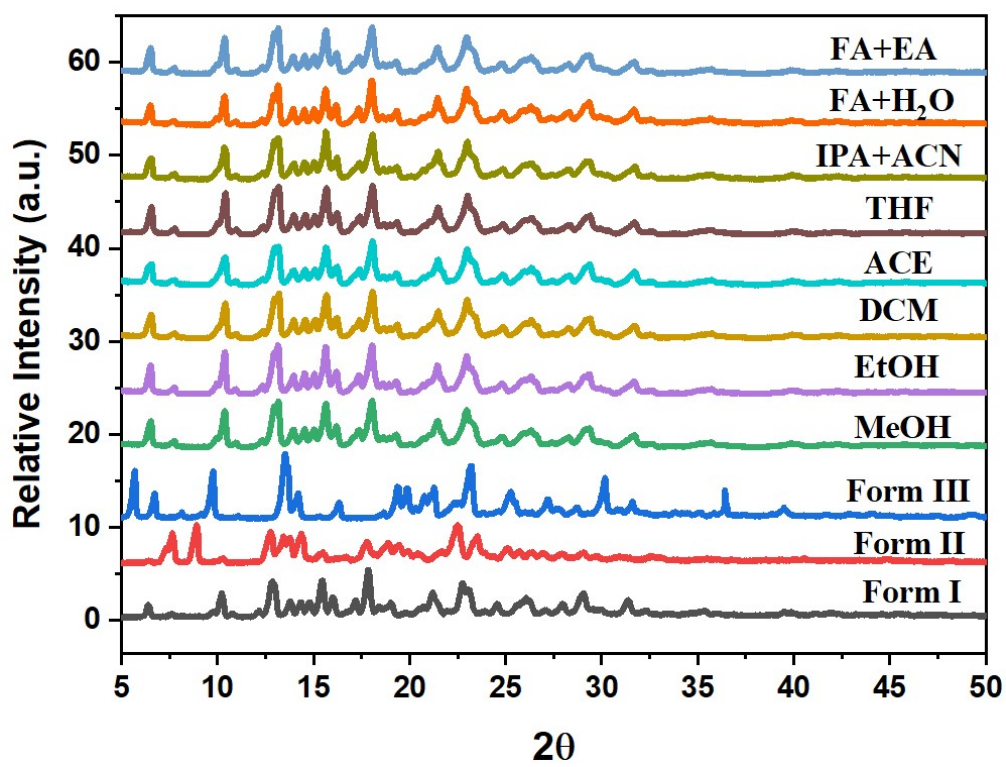
Figure S3. PXRD patterns of Form III.

Table S1. Distinctive X-Ray Diffraction Peaks in ENSE Polymorphs.

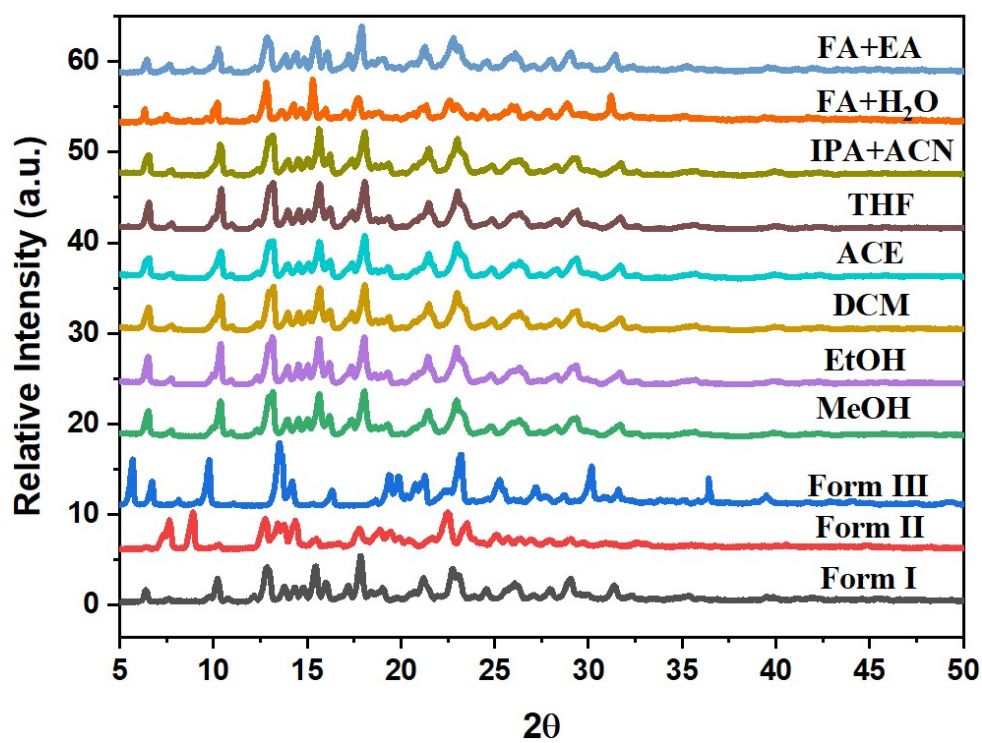
Polymorphic form	Peaks [2θ (deg)]
Form I	6.4, 10.2, 12.8, 13.8, 14.6, 14.8, 15.4, 16.1, 17.2, 17.9, 19.1, 21.2, 22.8, 24.5, 26.1, 27.9, 29.1, 31.5
Form II	7.6, 8.9, 10.3, 12.8, 13.5, 14.4, 15.5, 17.8, 18.9, 19.5, 22.5, 23.5, 25.1, 25.7, 26.4, 27.1, 27.9, 29.1, 29.8, 30.9, 32.5
Form III	5.6, 6.7, 9.7, 13.5, 14.2, 16.3, 19.4, 19.9, 20.7, 21.3, 23.2, 25.3, 27.2, 27.8, 28.7, 30.2, 31.6, 36.4, 39.5



(a)



(b)



(c)

Figure S4. Illustration of the formation of distinct forms under varied reaction environments. (a) rotary evaporation, (b) liquid-assisted grinding (LAG) and (c) LAG followed by slow-evaporation.

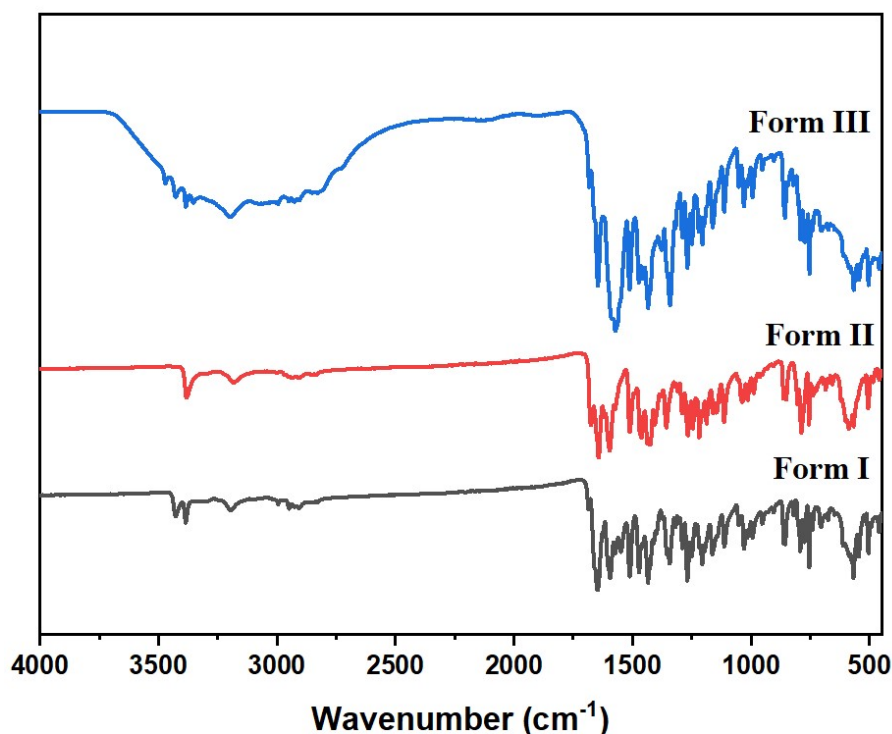


Figure S5. FT-IR spectra of various forms of ENSE.

¹H and ¹³C data of ENSE Forms

Form I

¹H NMR (400 MHz, DMSO-*d*₆) δ ppm: 6.97 (s, 1H), 6.86 (s, 2H), 6.67 (s, 1H), 6.11 (t, *J* = 5.8 Hz, 1H), 5.46 (s, 2H), 5.33 (s, 1H), 4.19 (t, *J* = 6.8 Hz, 2H), 3.92 (t, *J* = 6.0 Hz, 2H), 3.81 (s, 3H), 3.62 (s, 3H), 3.18 (d, *J* = 5.2 Hz, 1H), 2.91 (t, *J* = 5.9 Hz, 2H), 2.23 (s, 3H), 1.98 (s, 6H).

¹³C NMR (101 MHz, DMSO-*d*₆) δ ppm: 159.10, 152.19, 151.45, 148.64, 148.29, 144.53, 142.78, 131.07, 130.77, 128.86, 128.20, 119.36, 111.84, 109.05, 88.17, 56.55, 56.20, 41.97, 37.36, 27.50, 20.91, 18.49.

Form II

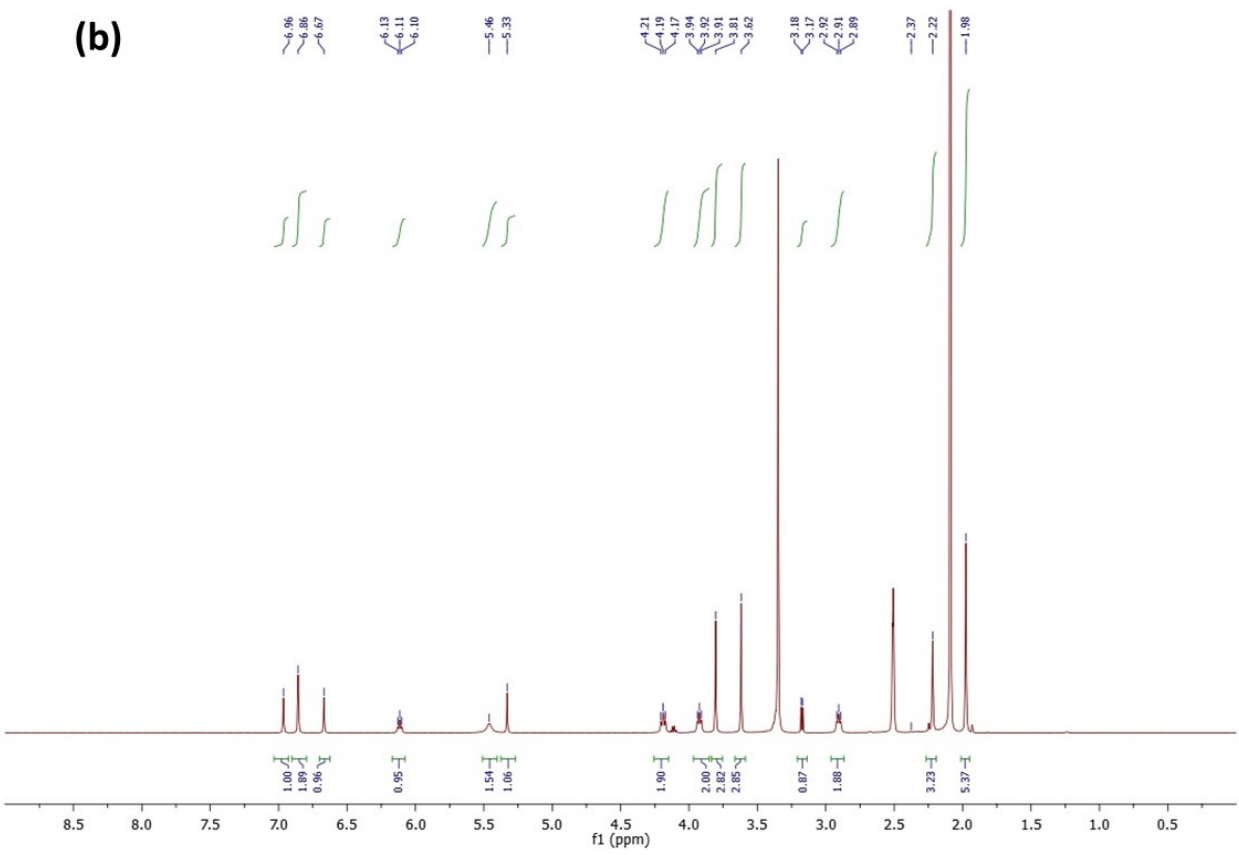
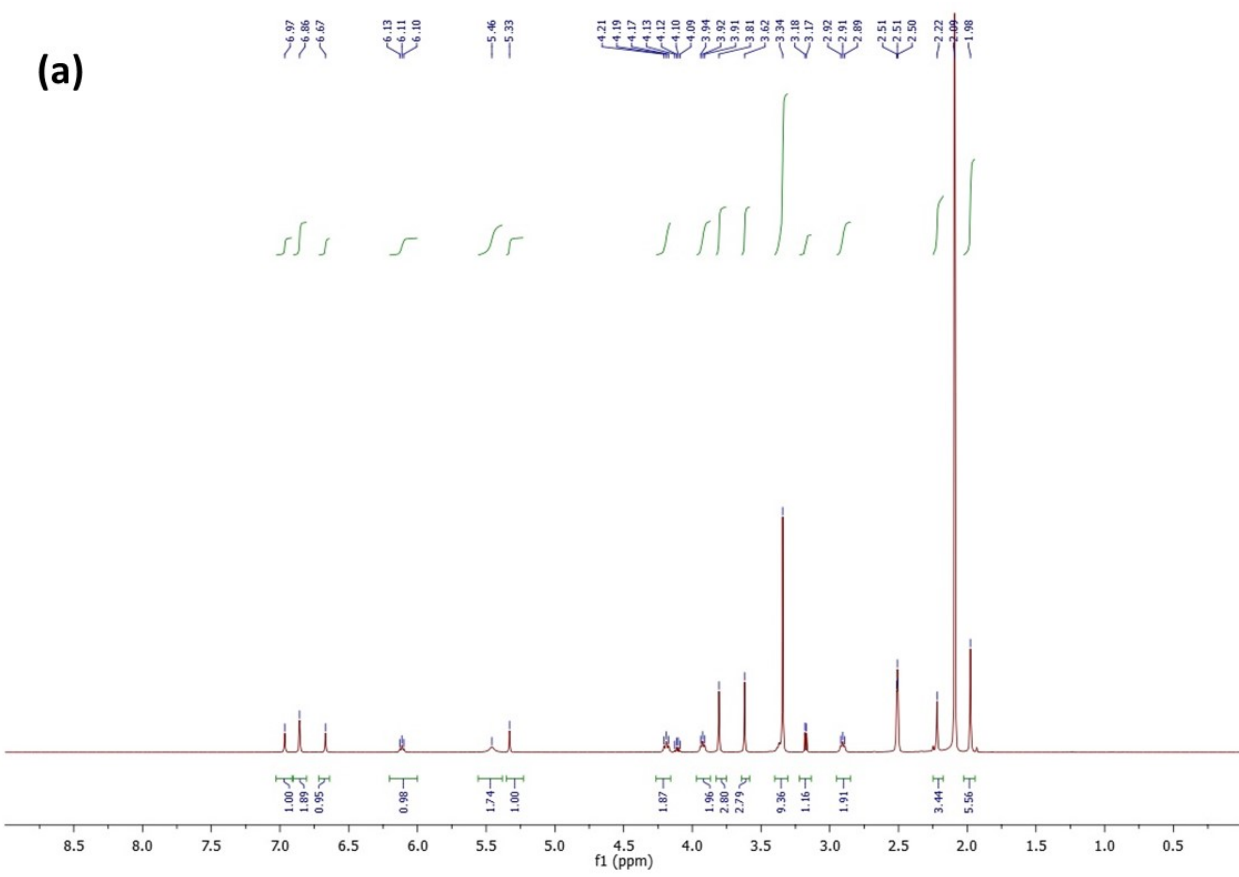
¹H NMR (400 MHz, DMSO-*d*₆) δ ppm: 6.97 (s, 1H), 6.86 (s, 2H), 6.67 (s, 1H), 6.11 (t, *J* = 5.8 Hz, 1H), 5.46 (s, 2H), 5.33 (s, 1H), 4.19 (t, *J* = 6.8 Hz, 2H), 3.92 (t, *J* = 6.0 Hz, 2H), 3.81 (s, 3H), 3.62 (s, 3H), 3.18 (d, *J* = 5.2 Hz, 1H), 2.91 (t, *J* = 5.9 Hz, 2H), 2.22 (s, 3H), 1.98 (s, 6H).

¹³C NMR (101 MHz, DMSO-*d*₆) δ ppm: 159.10, 152.20, 151.45, 148.64, 148.30, 144.53, 142.78, 131.07, 130.77, 128.86, 128.21, 119.36, 111.85, 109.06, 88.17, 56.56, 56.20, 41.97, 27.51, 20.91, 18.49.

Form III

¹H NMR (400 MHz, DMSO-*d*₆) δ ppm: 6.96 (s, 1H), 6.85 (s, 2H), 6.67 (s, 1H), 6.11 (t, *J* = 5.8 Hz, 1H), 5.45 (s, 2H), 5.33 (s, 1H), 4.19 (t, *J* = 6.8 Hz, 2H), 3.91 (t, *J* = 6.5 Hz, 2H), 3.80 (s, 3H), 3.62 (s, 3H), 3.37 (d, *J* = 6.3 Hz, 2H), 2.90 (t, *J* = 5.9 Hz, 2H), 2.22 (s, 3H), 1.97 (s, 6H).

¹³C NMR (101 MHz, DMSO-*d*₆) δ ppm: 159.09, 152.21, 151.45, 148.65, 148.31, 144.54, 142.78, 131.08, 130.76, 128.86, 128.20, 119.37, 111.86, 109.09, 88.17, 56.57, 56.21, 41.98, 37.37, 27.51, 20.91, 18.49.



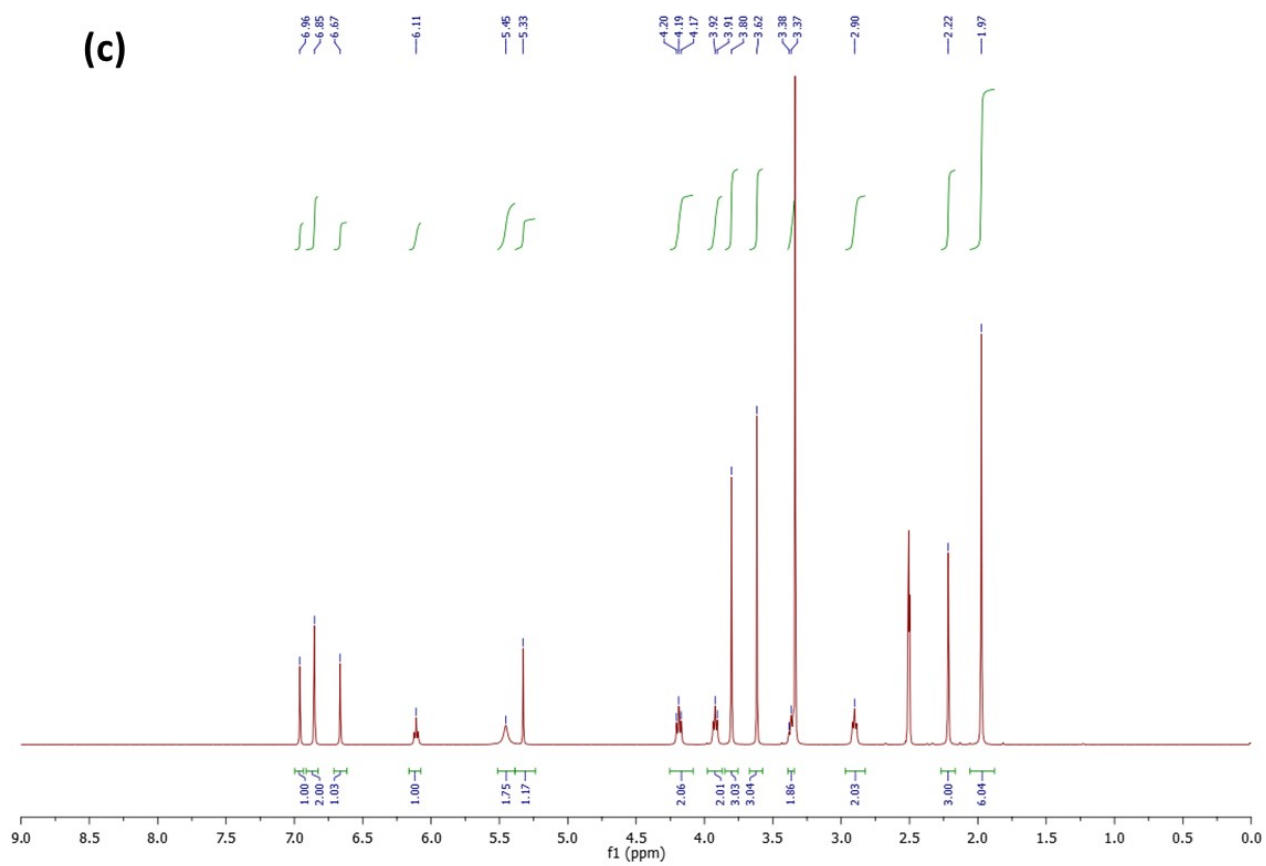
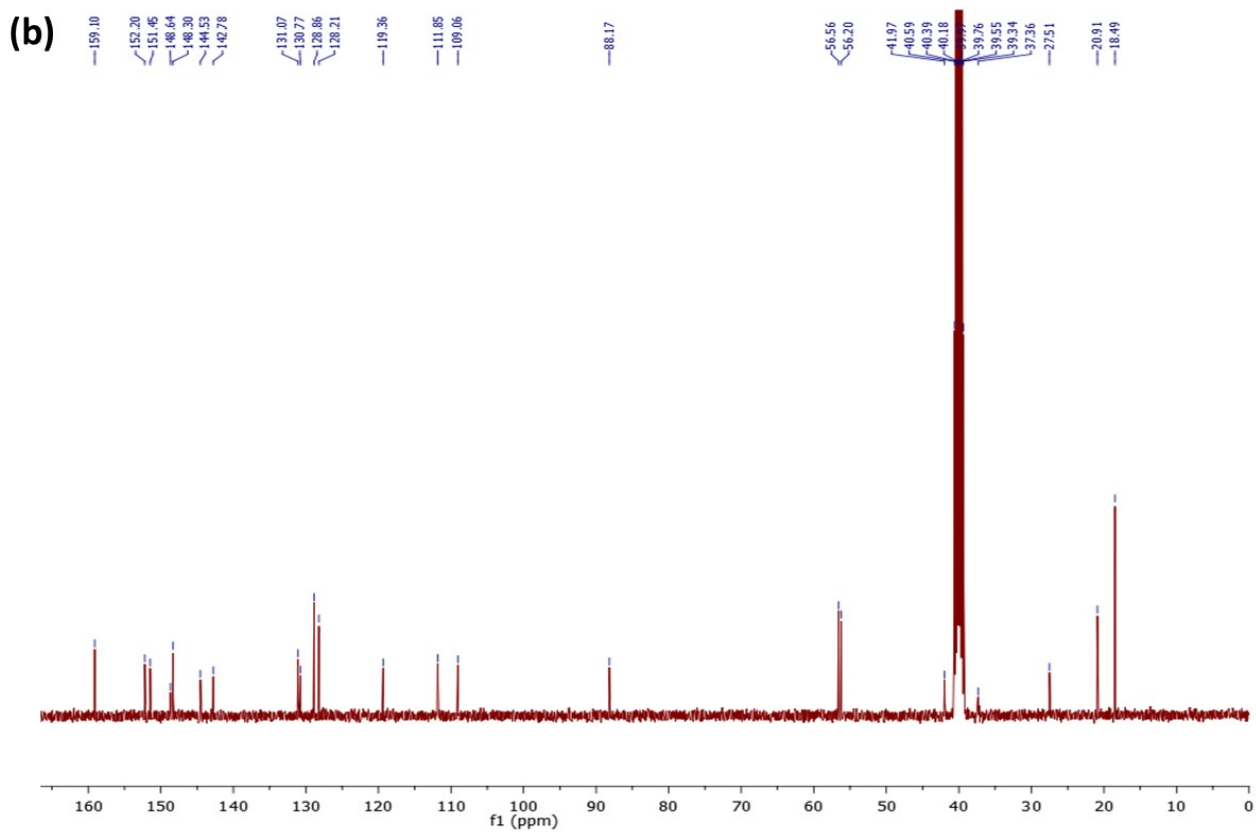
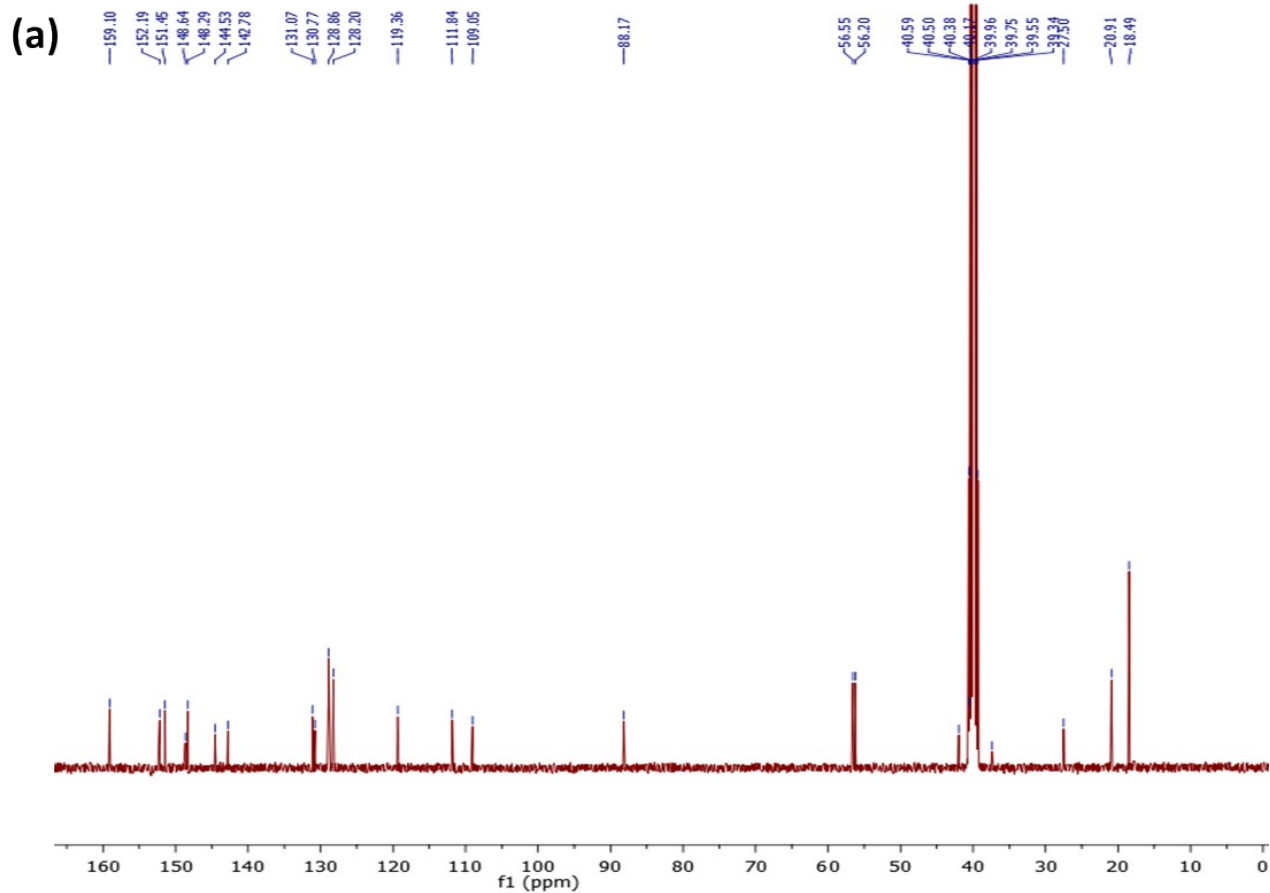


Figure S6. ¹H Spectra of (a) Form I, (b) Form II, and (c) Form III.



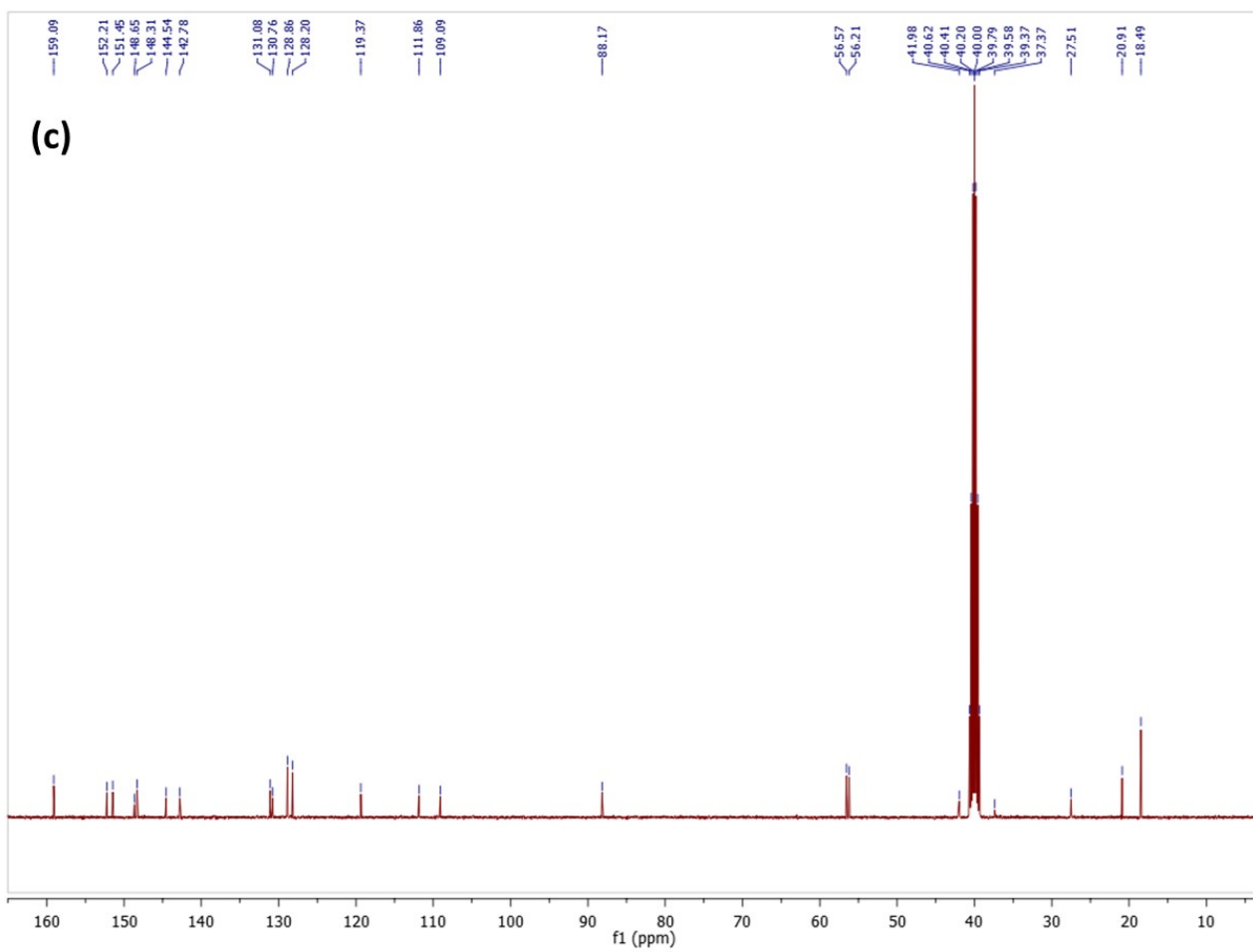


Figure S7. ^{13}C Spectra of (a) Form I, (b) Form II, and (c) Form III.

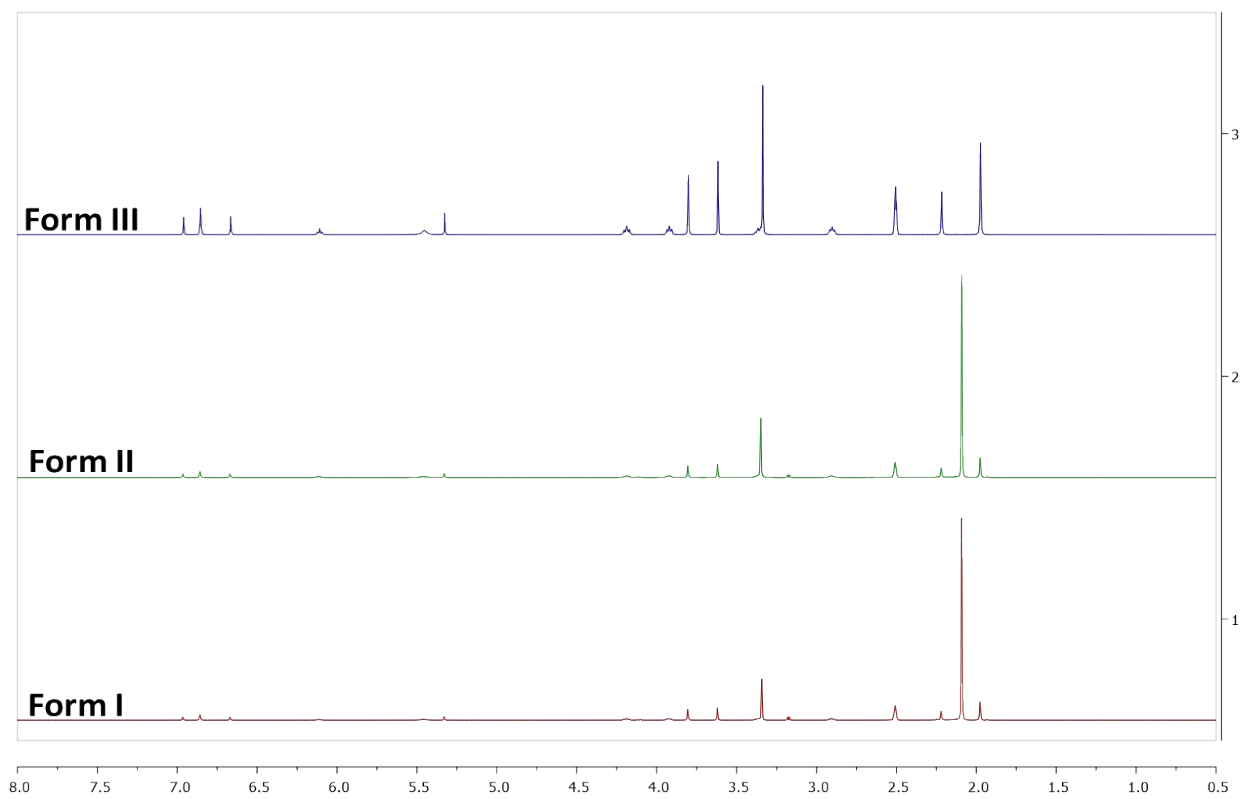


Figure S8. ¹H spectra overlay of all ENSE forms.

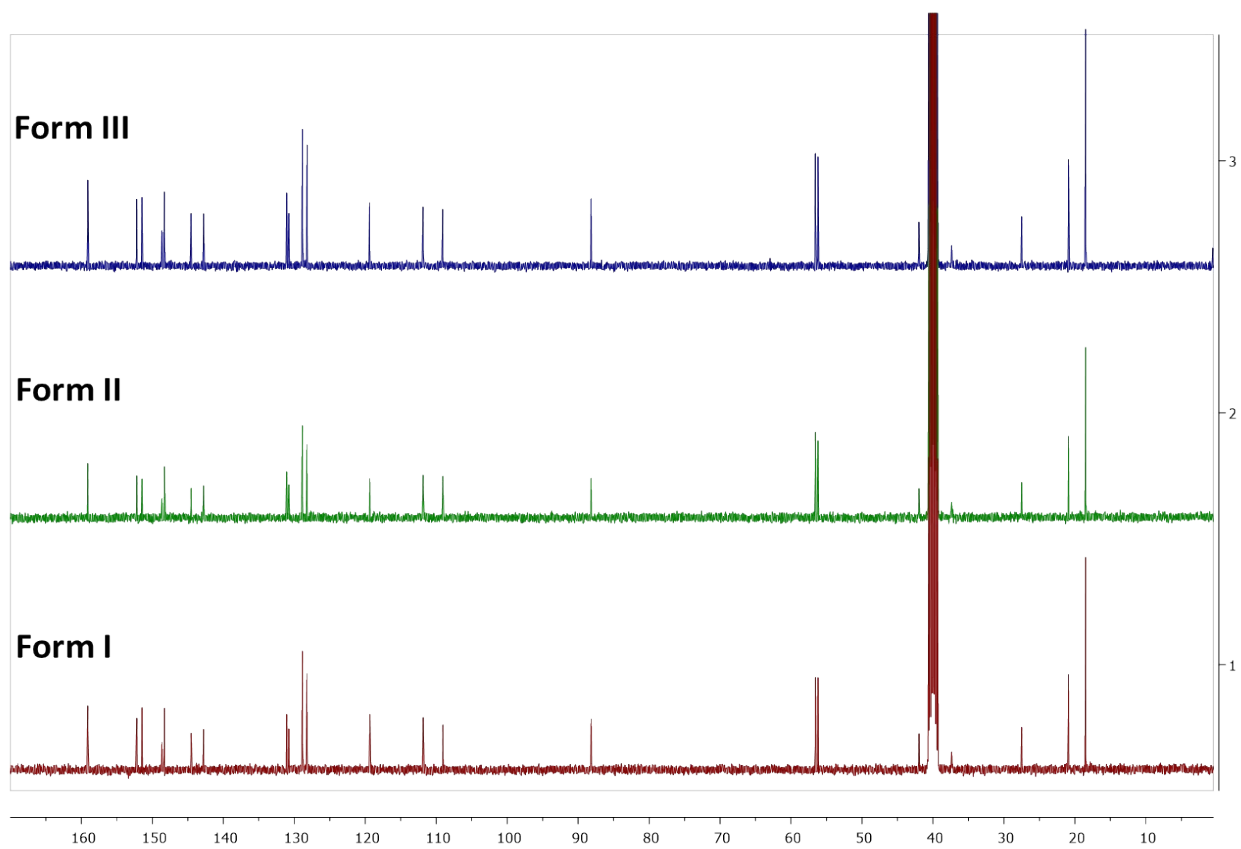


Figure S9. ^{13}C spectra overlay of all ENSE forms.

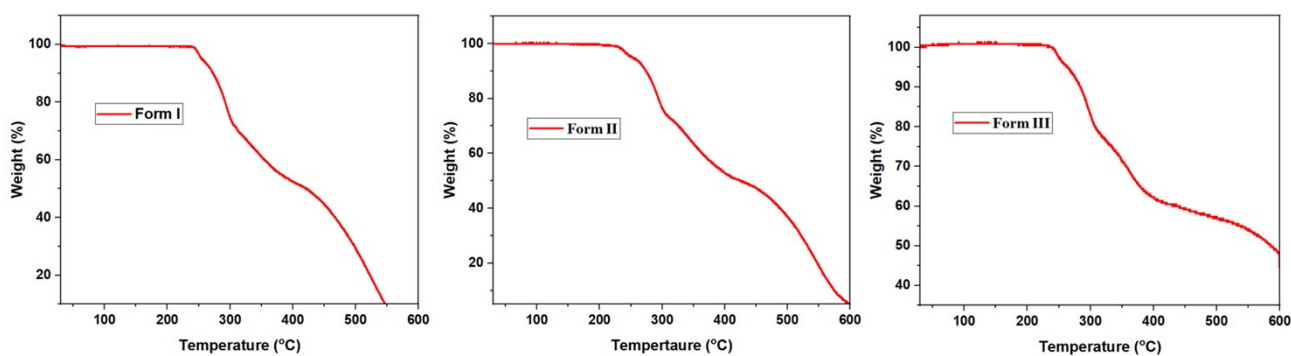
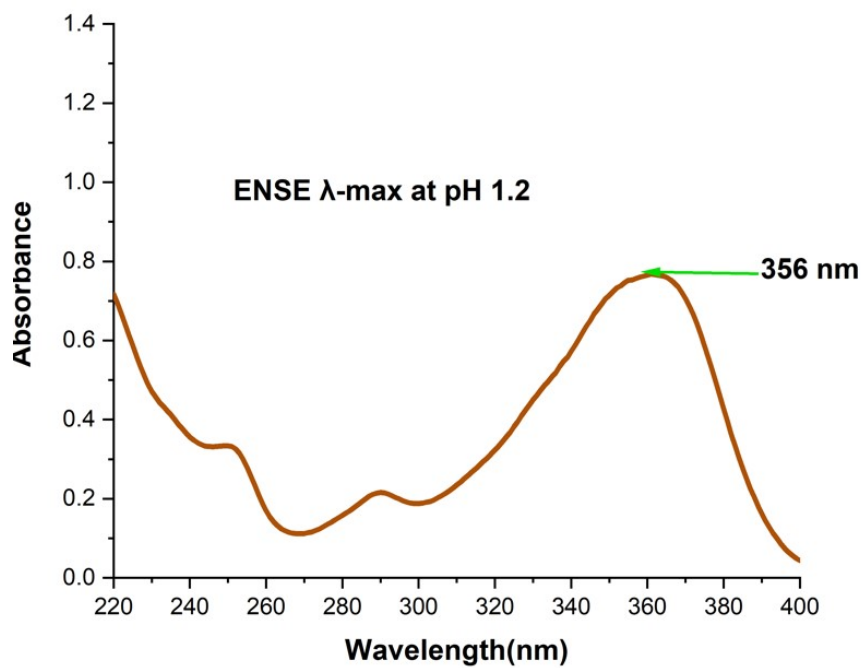
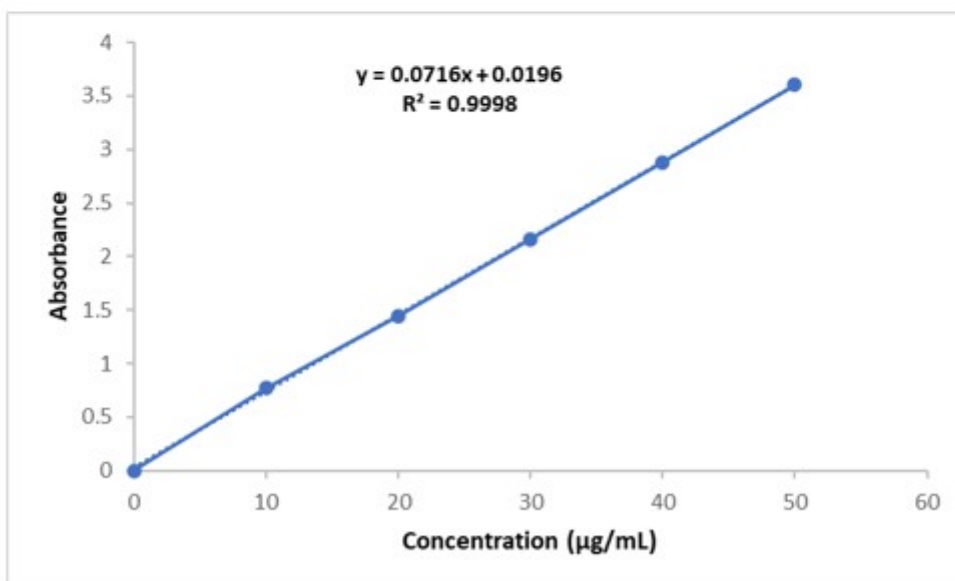


Figure S10. TGA profiles of various forms of ENSE.

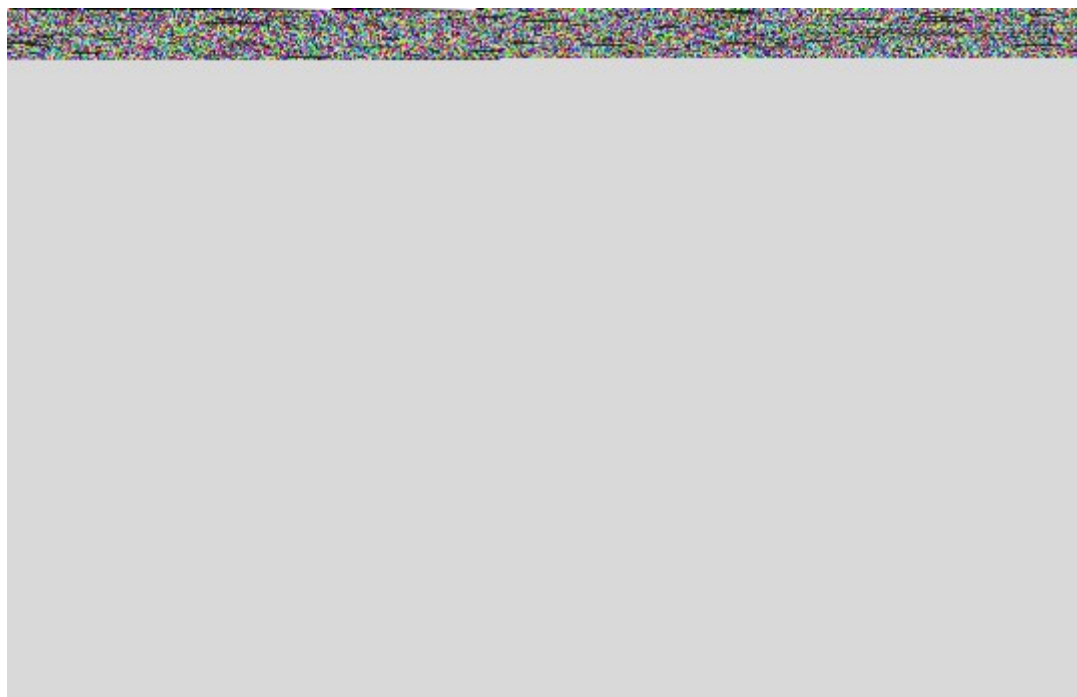
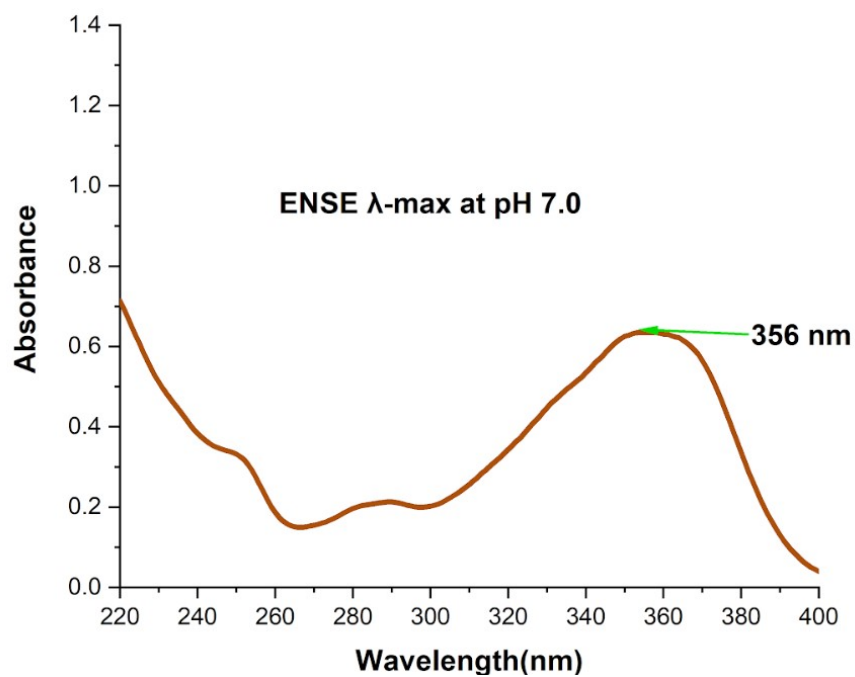
Details of the solubility parameters of solid forms of ENSE





Calibration graph of ENSE at pH 1.2.

S.No.	Sample Name	Absorbance			Estimated Standard Deviation	Average Absorbance	Average Concentration (mg/mL)	Final solid phase
1	Form I	1.436	1.432	1.435	0.002	1.434	19.795	SALT
2	Form II	0.06	0.04	0.05	0.01	0.05	0.6941	Form I
3	Form III	0.012	0.013	0.014	0.001	0.013	0.1753	Form I



S.No.	Sample Name	Absorbance			Estimated Standard Deviation	Average Absorbance	Average Concentration (mg/mL)	Final solid phase
1	Form I	1.886	1.883	1.885	0.002	1.884	0.029	Form I
2	Form II	0.242	0.241	0.246	0.003	0.243	0.004	Form I
3	Form III	1.175	1.179	1.18	0.003	1.177	0.741	Form I

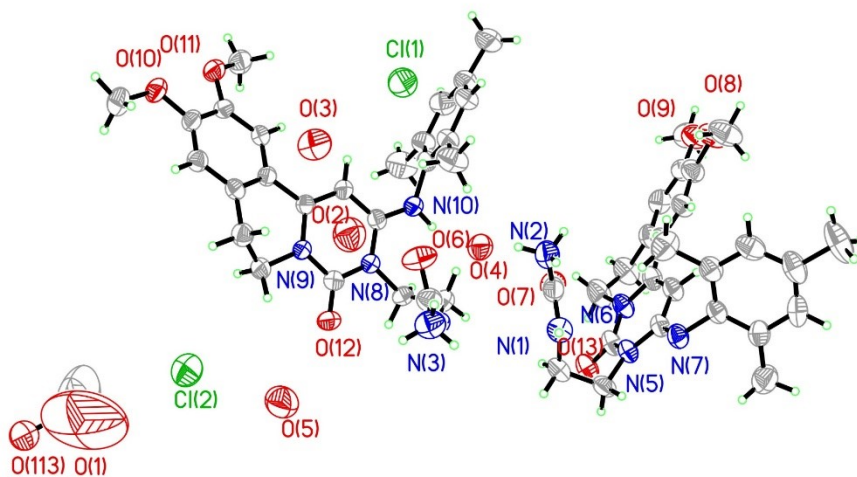


Figure S11. ORTEP view of ENSE.Cl Salt. Herein, the ellipsoids are drawn with a 50% probability.

Table S2. Crystallographic Parameters of ENSE.Cl.Salt.

Parameters	ENSE.SALT
Formula	2(C ₂₆ H ₃₂ N ₅ O ₄). 1(C O). 2(Cl). 4(O)
M_r	1120.04
crystal shape	Needle
crystal colour	Colorless
crystal system	Triclinic
space group	$P\bar{1}$
T , K	273(2)
λ (Mo-K α)/Å	0.71073
a /Å	12.371(8)
b /Å	13.385(7)
c /Å	17.690(2)
α ⁰	93.64(1)
β ⁰	105.06(2)
γ ⁰	91.16(1)
V /Å ³	2821(2)
Z	2
D_c / g cm ⁻³	1.319
μ , mm ⁻¹	0.186

2θ range [$^{\circ}$]	2.24-27.60
limiting indices	$-16 \leq h \leq 16$ $-17 \leq k \leq 17$ $-23 \leq l \leq 23$
$F(000)$	1180
total reflections	54109
unique reflections	13090
reflection at $I > 2\sigma(I)$	5756
No. of parameters	728
$R_1, I > 2\sigma(I)$	0.0751
$wR_2, I > 2\sigma(I)$	0.2536
GoF on F^2	1.110
CCDC No.	2349985

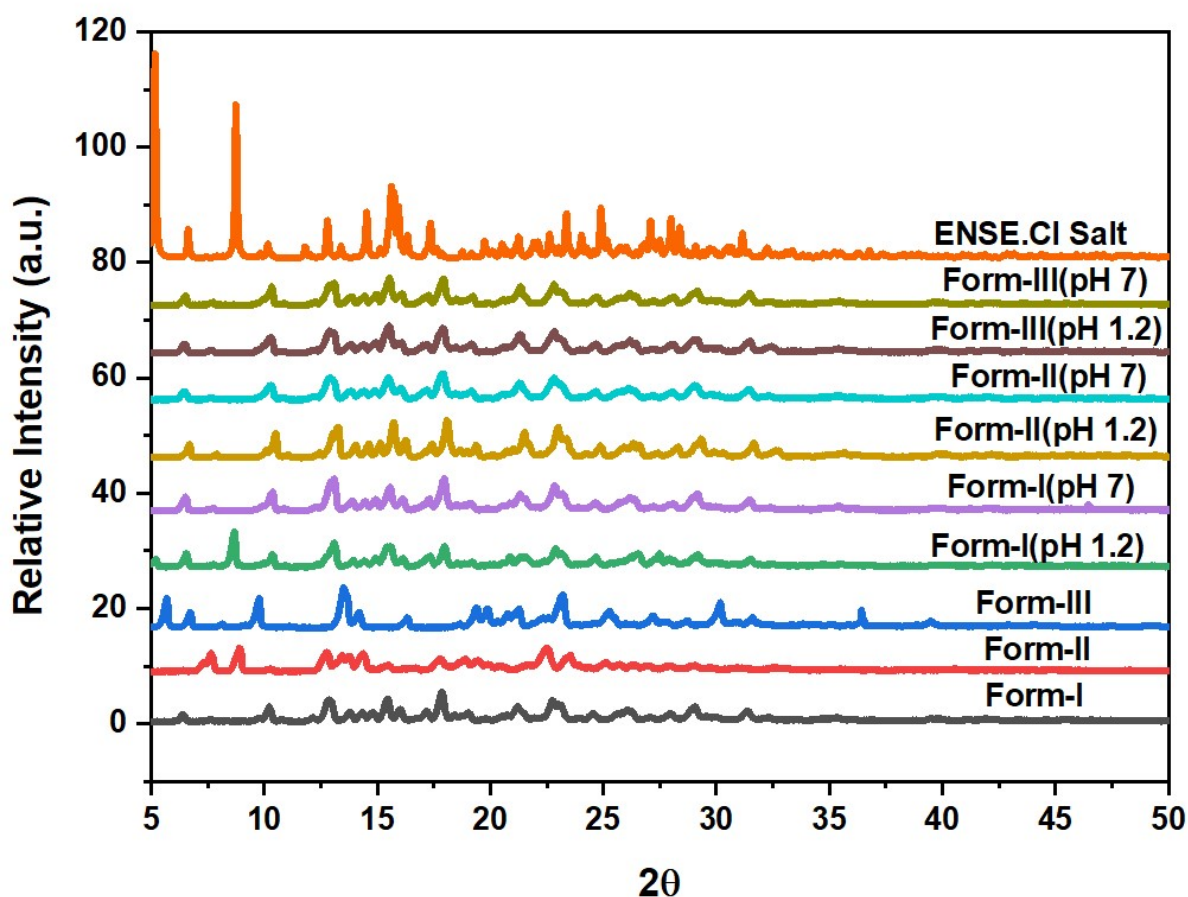


Figure S12. After the solubility test, a comparative PXRD overlay of all the solid forms of ENSE showed the production of discrete, stable adducts that matched the simulated pattern of ENSE.Cl Salt.